Transplant International

Transplant International ISSN 0934-0874

ORIGINAL ARTICLE

Piroxicam and meloxicam ameliorate hepatic oxidative stress and protein carbonylation in Kupffer and sinusoidal endothelial cells promoted by ischemia–reperfusion injury

Eduardo E. Montalvo-Javé,[1,2,4,5] José A. Ortega-Salgado,[1] Andrés Castell,[3] Daniel Carrasco-Daza,[6] David Jay,[7] Roberto Gleason,[8] Eduardo Muñoz,[8] César Montalvo-Arenas,[3] Rolando Hernández-Muñoz[9] and Enrique Piña[2]

1 Departamentos de Cirugía, Universidad Nacional Autónoma de México (UNAM), Mexico City, Mexico
2 Bioquímica, y, Universidad Nacional Autónoma de México (UNAM), Mexico City, Mexico
3 Biología Celular y Tisular, Facultad de Medicina, Universidad Nacional Autónoma de México (UNAM), Mexico City, Mexico
4 División de Cirugía Experimental, Hospital General Dr. Manuel Gea González, Secretaría de Salud (SSA), Mexico City, Mexico
5 Servicio de Cirugía General, Unidad 304, Hospital General de México, SSA, Mexico City, Mexico
6 Servicio de Patología Quirúrgica y Molecular, Instituto Nacional de Pediatría (INP) Mexico City, México
7 Departments of Pharmacology and Pediatrics, University of Alberta, Edmonton, Alberta, Canada
8 Departmento de Estado Sólido, Instituto de Física, Universidad Nacional Autónoma de México (UNAM), Mexico City, Mexico
9 Departmento de Biología Celular, Instituto de Fisiología Celular (IFC), Universidad Nacional Autónoma de México (UNAM), Mexico City, Mexico

Keywords
electron paramagnetic resonance, ischemia–reperfusion injury, Kupffer cells, liver, nonsteroidal anti-inflammatory drugs, protein carbonylation, reactive oxygen species, sinusoidal endothelial cells.

Correspondence
Enrique Piña MD, PhD, Departamento de Bioquímica, Facultad de Medicina, Universidad Nacional Autónoma de México (UNAM), Circuito Universitario 3000, Delegación Coyoacan, C.P. 04510 México, D.F., México. Tel.: 52-55-5622-0829; fax: 52-55-5616-2419; e-mail: epgarza@servidor.unam.mx

Conflicts of Interest
The authors have declared no conflicts of interest.

Received: 1 October 2010
Revision requested: 19 October 2010
Accepted: 15 December 2010
Published online: 25 January 2011

doi:10.1111/j.1432-2277.2010.01214.x

Summary

The present study was aimed to assess the effect of protein carbonylation (PC) in hepatic cells and effects of nonsteroidal anti-inflammatory drugs (NSAIDs) on indicators of tissue damage induced by liver ischemia–reperfusion injury (LIRI). Warm ischemia was performed by partial vascular occlusion during 90 min in Wistar rats. In serum, we determined the catalytic activity of Alanine Aminotransferase, Aspartate Aminotransferase, Lacticate Dehydrogenase, and Ornithine Carbamoyltransferase. In liver samples, we studied cellular alterations by means of histologic studies, lipid peroxidation, PC by immunohistochemistry, apoptosis and reactive oxygen species in bile by electron paramagnetic resonance. Based on PC data, sinusoidal endothelial cells (SEC) and Kupffer cells (KC) were the first to exhibit LIRI-associated oxidative damage and prior to parenchymal cells. Administration of piroxicam or meloxicam during the preischemic period produced a highly significant decrease in all studied injury indicators. No significant differences were revealed between the protective action of the two drugs. The data shown here suggest the potential use of NSAIDs such as piroxicam or meloxicam in minimizing ischemic event-caused damage in liver. We also propose that PC may be employed as an adequate tool to assess tissue damage after oxidative stress.

Introduction

Ischemia–reperfusion (IR) injury occurs when a tissue is temporarily deprived of blood supply and the return of the blood supply triggers an intense inflammatory response [1]. Liver ischemia–reperfusion injury comprises a complex phenomenon that occurs in many clinically important events, including hepatic surgery, transplantation, trauma, and hemorrhagic shock [2]. In this organ, sinusoidal endothelial cells (SEC) and Kupffer cells (KC) constitute a

coordinated defence system. The sieve-like plates of the endothelial cell cytoplasm and the absence of a structurally defined basement membrane (in contrast to capillaries) facilitate exchange between blood and hepatocytes [3]. The changes observed in SEC included vacuolization of the cytoplasm, and enlargement of fenestrae and blebs of the sinusoidal lumen [4,5]. The ischemia activates Kupffer cells (KC), which are the main sources of vascular reactive oxygen formation during the initial reperfusion period [6]. A burst of reactive oxygen species (ROS) occurs on restoration of blood flow after an ischemia–reperfusion injury [7]. Moreover, KC generate primary cytokines such as tumor necrosis factor-alpha (TNF-α) and interleukin-1 (IL-1), tumor necrosis factor-beta (TNF-β), interferon gamma (IFN-γ), and granulocyte colony-stimulating factor (GCSF), which enhance KC activation and promote neutrophil recruitment into the liver [8,9]. After the reperfusion, injury is aggravated with death of SEC by apoptosis, adherence, and activation of neutrophils, lymphocytes, and platelets [10,11]. As part of this inflammatory response, arachidonic acid metabolites such as thromboxane A2 (Tx), prostaglandins (PGs), and leukotrienes are released [12]. The effects of Tx on LIRI are characterized by stimulating neutrophil aggregation and recruitment and inducing platelet aggregation; both activities promote vasoconstriction and increase vascular permeability, leading to edema and thrombosis [13]. The effects of PG on IR-subjected liver include, among others, inhibition of ROS generation, improvement in insulin action and lipid metabolism, prevention of leukocyte migration, reduction in synthesis or production of membrane degradation products, regulation cell adhesion molecules, and hepatocyte (HEP) proliferation [14]. As a whole, these inflammatory responses and microcirculatory alterations further aggravate the injury after reperfusion [15,16].

Moreover, ROS have been suggested to be the primary activators of the mitochondrial permeability transition pore, a large multiprotein conductance channel. The opening of this channel causes a loss in membrane potential, mitochondrial swelling with membrane rupture, cytochrome C release, and apoptosis [17,18].

The generation of protein carbonyls is formed by a direct metal-catalyzed oxidative attack on the amino acid side chains of proline, arginine, lysine, and threonine. In addition, carbonyl derivatives on lysine, cysteine, and histidine can be formed by secondary reactions with reactive carbonyl compounds on carbohydrates (glycoxidation products), lipids, and advanced glycation/lipoxidation end-products [19]. Some diseases have been associated with PC, such as Alzheimer, Parkinson, diabetes, sepsis, cancer, and others [20–22].

Prostaglandin synthase, also known as cyclooxygenase (COX), is the key and first regulatory enzyme in the arachidonic cascade leading to PG, Tx, and prostacyclin syntheses [23]. The COX enzyme exists in two isoforms: COX-1, a constitutive form that is expressed in multiple cell types and that is generally considered to contribute to the normal tissue homeostasis maintenance [24], and COX-2, an inducible form that is rapidly up-regulated in response to lipopolysaccharides, cytokines, and mitogens and that is found more commonly in inflammatory and immune cells [25]. Tx and PG production through both COX isoforms is inhibited by nonsteroidal anti-inflammatory drugs (NSAIDs) such as piroxicam and meloxicam. Piroxicam is a preferential COX-1 inhibitor [26] and meloxicam is a better COX-2 inhibitor [27]; both are widely used in the clinical setting and are non-specific blockers of Tx or PG pathways [12]. Based on all the information provided, it appears reasonable to assay the role of NSAIDs in restraining the inflammatory response observed after LIRI. A previous study by our group showed a beneficial action of aspirin, naproxen, nimesulide, and piroxicam in an alternative model of hepatic ROS generation such as acute ethanol intoxication; these NSAIDs prevented hepatic increase in lipids and thiobarbituric-acid reactive substances (TBARS), protein carbonylation (PC) [28], and the decrease in glutathione produced after ethanol ingestion [29–32]. Thus, the purpose of this study was to focus on evaluating the effect of PC on hepatic cells and the protective effects of piroxicam and meloxicam during a 24-h time course after reperfusion in a rat warm-ischemia model.

Materials and methods

Animals

After approval by the Animal Care and Ethics Committee of the Mexico City-based Hospital General Dr. Manuel Gea González, we used male Wistar rats weighing 250–300 g that were obtained from the Animal Facility, Universidad Nacional Autónoma de México (UNAM) School of Medicine, which were fed commercial rat chow (Purina, Cuautitlán, Estado de México, México) and water *ad libitum* under a 12-h dark–light cycle and maintained at a constant temperature of 22 °C.

Rats were randomly divided into four study groups (n = 10 for each time) as follows: Group I – sham (surgical procedure without vascular clamping); Group II – ischemia–reperfusion group without administration of any drug; Group III – animals subjected to the ischemia–reperfusion protocol and treated with piroxicam (13 mg/kg) (Senosiain, Celaya, Guanajuato, México); and Group IV – animals treated with meloxicam (0.9 mg/kg) (Boehringer Ingelheim, Xochimilco, México D.F., México). Drugs were administered intraperitoneally (IP) 1 h before surgery.

A warm hepatic ischemia/reperfusion model was utilized. Arterial and portal venous blood supplies were interrupted during 90 min to cephalad lobes of liver employing a vascular atraumatic clamp in groups II, III, and IV, followed by a variable reperfusion time. Samples for specific determinations were taken at 0.5, 1, 1.5, 2, 4, 12, and 24 h during the reperfusion period.

Surgical procedure

After a 12-h fasting period, with water *ad libitum*, under general anesthesia with xylazine (100 mg/kg) and ketamine (13 mg/kg) (Pisa, Guadalajara, Jalisco, México), rats were placed in dorsal decubitus and the peritoneal cavity was dissected by means of a longitudinal incision by plane utilizing bipolar electrocautery. After dissection and gut mobilization to the right, portal vein, hepatic duct, and hepatic artery were identified and subjected to ischemia using a microvascular clamp (Braun-Aesculap, Tuttlingen, Germany), interrupting the hepatic blood flow. After 90 min of partial hepatic warm ischemia, the clamp was removed, initiating hepatic reperfusion. During the surgical procedure, the animals were maintained hydrated IP with an isotonic saline solution at 36.5 °C at a flow of 15 ml/kg/h; throughout the surgical procedure and recovery, rats were placed on a neonatal thermal pad at 36.5 °C to avoid hypothermia. Liver samples were taken from the right lateral and median lobe for analytical procedures. The abdominal cavity was closed in planes using a Polyglactin 910 5-0 gastrointestinal suture (Ethicon-J&J, NY, USA). Animals placed on the neonatal thermal pad were monitored during their postoperative period for the following 4 h and were then placed into the animal fence-in for 24 h.

Assessment of hepatic function

Blood samples were taken from suprahepatic veins 0.5–24 h after hepatic reperfusion to determine serum enzyme levels (activities) of Alanine Aminotransferase (ALT), Aspartate Aminotransferase (AST), Lacticate Dehydrogenase (LDH), and Ornithine Carbamoyltransferase (OCT). Each sample was placed in an Eppendorf tube and centrifuged at 5000 *g* for 10 min; the serum was obtained using a Pasteur pipette, transferred to new Eppendorf tubes, and processed routinely using a Universal Kit (Bayer, Leverkusen, Germany); OCT activity was determined by the method of Ceriotti [33].

Histopathologic study

Hepatic damage was assessed as a function of acinus and/or lobular affection, which has been well characterized in acute, sub-acute, and chronic hepatitis, as well as in hepatic ischemic injury [34,35]. In fixed paraffin-embedded liver samples, we assessed the following variables: hepatocellular necrosis; congestion and vascular ectasia; and type and amount of inflammatory infiltrate. We used a conventional scale: minimal (<25%); moderate (25–50%), and severe (>50%). Determinations were performed in a minimum of 10 portal spaces chosen at random. The stains utilized were those considered as routine for evaluation of hepatic damage and consisted of hematoxylin–eosin (H&E), Masson, and Periodic acid-Schiff (PAS) with and without diastase.

Thiobarbituric reactive substances (TBARS) assay

Liver homogenates (1:3 w/v) in PBS buffer (pH 7.4) were obtained from hepatic samples of each experimental group. After filtration, homogenates were incubated at 37 °C under shaking for 30 min. At the end of incubation, 20% acetic acid (Sigma, St. Louis, MO, USA) and 0.8% thiobarbituric acid (Sigma Chemicals Co., St. Louis, MO, USA), previously dissolved in phosphate buffer were added. The mixture was boiled for 45 min to complete the chemical reaction, covering the tubes with marbles to avoid evaporation. The developed color was obtained with 15:1 n-butanol–pyridine (Sigma), mixed, and centrifuged at 5000 *g*. Finally, the pink-colored supernatant was read at 532 nm in a Beckman-650 photometer (Beckman, Brea, CA, USA). Protein was determined according to the Bradford method for calculating TBARS per milligram of protein [31,36].

Electron paramagnetic resonance (EPR) in bile samples

Intravenous (IV) administration (through portal vein) of the spin trap alpha-phenyl *N*-tert-butylnitrone (PBN) [700 mg/kg in dimethyl sulfoxide (DMSO)] was carried out 5 min prior to reperfusion. Bile samples (1.5–2.0 ml each) were collected by placing a PE-23 (tubing) cannula (Becton Dickson & Co., Sparks, MD, USA) into common bile duct, and bile was sequentially collected over the following 120 min ($n = 5$ per group). Bile samples were then frozen in liquid nitrogen and stored at −70 °C until EPR measurements were taken. Thawed bile samples were transferred into flat quartz EPR cells (model WG-812; Wilmad LabGlass, Vineland, NJ, USA) and studied in an EPR spectrometer (e-Line Century Series provided by Varian, Palo Alto, CA, USA). Typical EPR operating conditions were as follows: gain, 5×10^4; modulation amplitude, 2.0 G; modulation frequency, 100 kHz; microwave power, 2 mW; and time constant, 0.5 min, while sweep time for each spectrum was recorded for 4 min at room temperature. Ten scans were typically accumulated (we

observed no change in signal intensity during data accumulation) to average out and intensify the weak signals observed, which were first detected using an Agilent model 54622A oscilloscope (Agilent, Santa Clara, CA, USA). Excel Microsoft software was employed to process data. Relative EPR signal intensities were assessed by measuring the height of EPR peaks in millimeters under the spectrometer conditions mentioned previously.

Immunohistochemistry of protein carbonylation

Rate of oxidized protein was followed through an immunohistochemical (IHCh) reaction, for which a biotin–streptavidin–peroxidase complex method was used. Tissues were fixed in ethanol for 2 h and then embedded in paraffin. Sections of 2 mm and 3 mm were made and immunostaining was achieved with the marked polymer technique using EnVision HRP+ (DAKO Corp., Carpinteria, CA, USA). To modify the antibody-binding site, we employed 0.1% of 2,4-dinitrophenylhydrazine (Sigma Chemical Co.) in 2 N HCl. Samples were treated with 0.3% H_2O_2 in aqueous medium for 5 min to block endogenous peroxidase activity. Samples were treated with 1% bovine serum albumin dissolved in PBS for 5 min to eliminate unspecific binding sites. They were then incubated for 45 min with the anti-DNP (1:1) monoclonal antibody (Zymed-Invitrogen, San Francisco, CA, USA), followed by the addition of peroxidase-conjugated polymer and antimouse secondary antibody for 30 min. To visualize the reaction, 3,3′-diaminobenzidine–H_2O_2 (DAKO Corp.) was used as substrate. As negative control, we used normal mouse serum in PBS instead of the primary antibody. The whole tissue was immunohistochemically analyzed. Positive and negative interpretation was based on standard criteria consisting of a staining affinity of <10% of the cell population with specific immunolocalization (membrane staining), and staining intensity was considered as follows: +, weak; ++/+++, moderate; and ++++, intense. Positive control for IHCh mounting technique was performed with cerebral tissue of one patient with Alzheimer disease according to the technique published by Smith *et al.* [37].

Immunohistochemistry of CD34 and -68

For immunohistochemical studies, 2-μm-thick sections were treated with 0.1 M sodium citrate (pH 6.0) and Tween 20 for unraveling of epitopes. Endogenous peroxidases were blocked with 0.3% hydrogen peroxide, followed by incubation with 1% bovine serum albumin in PBS for 5 min to eliminate nonspecific binding. Monoclonal antibodies were used against CD34 (clone QBEnd 10; DAKO), dilution 1:50 in this study. The sections were incubated with primary antibodies for 45 min. After the primary antibodies, the sections were incubated for 30 min with biotinylated antimouse/antirabbit antibody followed by a similar incubation with the streptavidin/peroxidase complex (LSAB + Labeled streptavidine-Biotin HRP; DAKO). The reaction products were visualized with 3,3′-diaminobenzidine–H_2O_2 and subsequently washed with PBS buffer for 4 min. The sections were also incubated with ab CD68 (clone PG-M1; DAKO), dilution 1:150. Sections were then incubated with biotinylated antimouse/antirabbit antibody and with the streptavidin/phosphatase alkaline complex for 30 min each (LSAB + Labeled streptavidine-Biotin PA; DAKO). Reaction products were visualized with substrate new fuchsin (Biogenex, Fremont, CA, USA). Sections were subsequently counterstained with Gill hematoxylin solution. Normal liver samples were used as positive controls; for negative control, PBS was substituted for primary antibodies.

Assessment of apoptosis by light microscopic TdT-mediated dUTP nick-end labeling (TUNEL) assay

Apoptosis was assessed by the detection of DNA fragmentation using *in situ* TUNEL assay by light microscopy. Liver slides were processed using an ApopTag *in situ* apoptosis detection kit (Intergen Co., Purchase, NY, USA) according to manufacturer's instructions. Briefly, liver tissue slides were pretreated with proteinase K and H_2O_2 and incubated with the reaction mixture containing terminal deoxynucleotidyl transferase (TdT) and digoxigenin-conjugated dUTP for 1 h at 37 °C. The labeled DNA was visualized with HRP-conjugated anti-digoxigenin antibody with diaminobenzidine as the chromogen. For negative control, the TdT enzyme was omitted from the reaction mixture. As described previously by Corona-Morales *et al.* [38], 10 portal spaces of each culture were randomly chosen, and positively stained cells were counted.

Statistics

The Kruskall–Wallis test was employed to assess whether differences existed among the studied groups. When statistically significant differences were revealed, the Mann–Whitney *U*-test was utilized to compare the studied groups in order to identify statistical differences with $P < 0.05$.

Results

Serum activity of liver enzymes

In this study, we used six different indicators of liver damage produced by ischemia–reperfusion; only one of

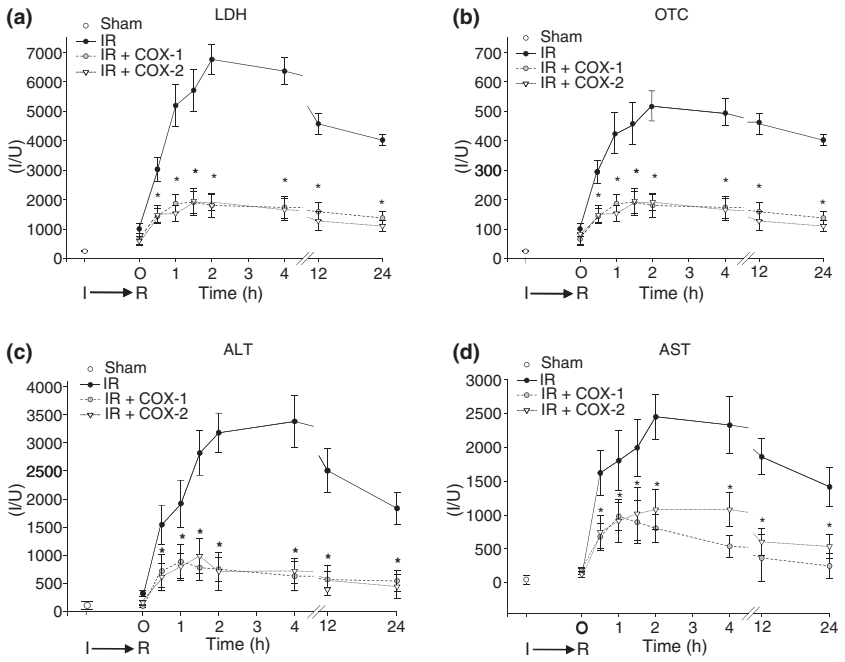

Figure 1 Serum values of liver enzymes activity. ALT, AST, LDH, and OCT patterns in a 24-h period; values are expressed in IU/l. Statistically significant differences at the different times tested are indicated by an asterisk ($P < 0.05$).

these, namely the serum enzymes assay, is regularly used in clinical practice. Thus, the Results section is herein initiated with the presentation of progressive changes in the serum activity of liver enzymes during the experimental protocol. The idea was to expedite a correlation between values of increased serum enzymes from the liver with the magnitude of liver damage observed after the assay with other indicators. Blood samples were taken from suprahepatic veins at different times after LIRI to assay the catalytic activity of released liver enzymes. The sham group (I) depicted normal serum values of liver enzymes during the experiment as shown in Fig. 1a; recorded values of the enzymes studied were substantially higher after 1-h reperfusion (Fig. 1b–d). The pattern of change in serum activity was similar for liver enzymes that are mainly present in cell cytosol (ALT, AST, and LDH) in comparison with enzymes localized within the mitochondrial space [39,40]. Either piroxicam or meloxicam treatment partially prevented, in similar fashion, the release of serum enzymes after 2, 4, and 12 h postreperfusion (Fig. 1).

Histologic changes

Liver ischemia–reperfusion injury-associated histologic changes followed tissue evolution described for many organs and systems subjected to a similar stress. During the ischemic period (90 min), no inflammatory cells, no damage to microcirculation (stasis), and no necrosis were observed in the three groups of IR-subjected animals. Once reperfusion had been initiated and at 60 min (1 h), the sole group affected was the nontreated IR group, which exhibited focal presence of apoptotic bodies, as well as edema and congestion. These findings were initially found in the COX-1-inhibited group (III) at 60 min and in the COX-2-inhibited group (IV) at 2 h, until reaching a plateau accompanied by the presence of inflammatory cells, apoptosis, and congestion. Necrosis appeared in the nontreated IR group beginning at 2 h, and at 4 h in both NSAIDs-treated groups and was absent at 12 h in the nontreated IR group, becoming bridges and remaining focal in piroxicam- and meloxicam-treated animals (Fig. 2).

Presence of ROS measured indirectly by TBARS and directly by EPR

Levels of TBARS, a widely used indicator of lipid peroxidation caused by the presence of ROS, were significantly higher in the IR group than in the sham group. In the case of piroxicam- and meloxicam-treated groups, both demonstrated reduced TBARS levels after IR compared with the IR group alone (Fig. 3a). In parallel fashion and as in the release of liver enzymes, there were significant differences in TBARS levels between untreated and treated groups, which were noted 4–8 h after reperfusion. No significant differences were found among the treated groups.

As shown in Fig. 3b, when bile samples were taken from the bile duct during the liver reperfusion phase to measure ROS pool directly, a decline in signal intensity in

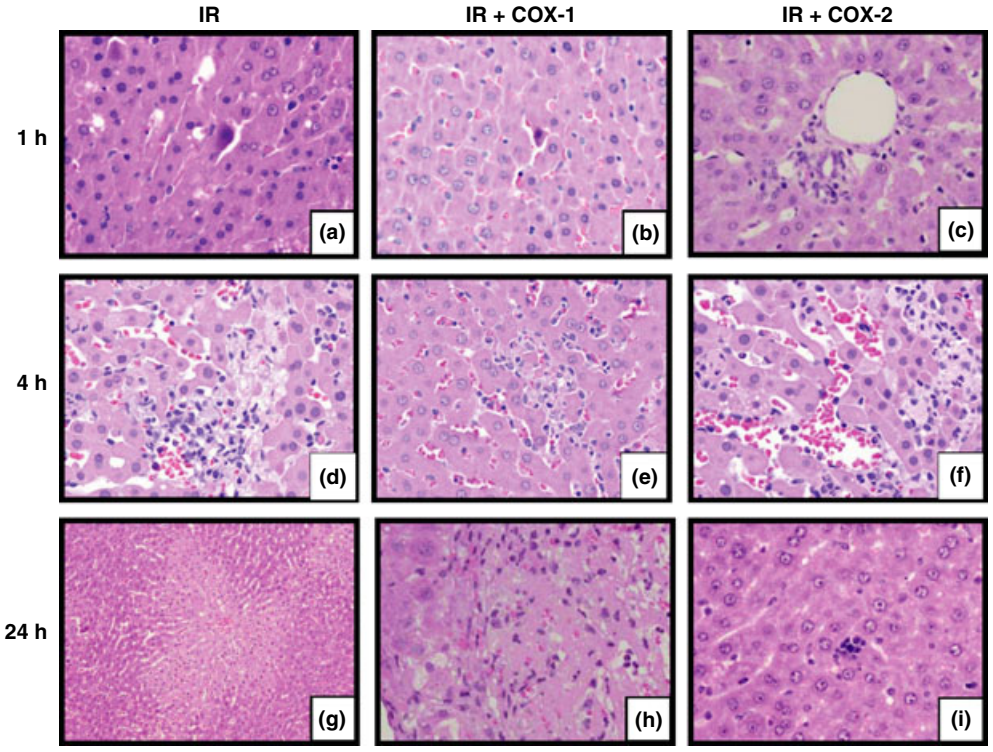

Figure 2 Representative hematoxylin–eosin staining of liver. After 1 h of reperfusion (a) showed apoptotic bodies (3) and minimal inflammatory cells. (b) Apoptotic body (1) without inflammatory cells. (c) Normal hepatic preservation. In contrast, after 4 h of reperfusion (d), liver samples exhibited focal necrosis areas and moderate inflammatory cells. (e) Focal necrosis and minimal inflammatory cells. (f) Lower focal necrosis. At 24 h of reperfusion, the ischemia–reperfusion group showed (g) dropout and severe necrosis. Samples from livers treated with COX-1 and -2 inhibitors (h, i) showed scant focal necrosis and fewer inflammatory cells. Original amplification, 10× and 20×.

NSAIDs-treated groups was observed compared with the nontreated IR group. No ROS presence was found in the sham group. However, a small paramagnetic signal could be detected in the majority of bile samples analyzed, including those from the sham group and those from treated and nontreated IR groups (see arrow in Fig. 3b). This spectral feature was detected even in the absence of PBN, indicating the presence of a small amount of a paramagnetic species in bile, and although its chemical nature could not be determined, this presented characteristics (isotropic, centered around $g = 2.0028$) associated with a nonmetal-centered free radical.

Protein carbonylation

Analysis of the PC phenomenon in the three IR groups at progressive times revealed that no PC generation occurred during the first 90 experimental minutes (ischemia time), with the exception of positive staining in Kupffer cells in group II (Fig. 4). In addition, positive PC appeared in SEC from the nontreated IR group, but not in NSAIDs-treated groups from the beginning of reperfusion. The same expression pattern was retained for the following 30–60 min, with only slight intensity changes and initial compromising of KCs. At 90 min, the three groups showed PC in the previously defined cells (SEC, KC, and HEP). Cell population number and PC signal intensity remained constant at 2 h and 4 h in the three groups; at 12 h, a disappearance of PC was observed, mainly in HEP. During the following 12 h and up to 24 h after initiating perfusion, PC was absent in HEP and KC in COX-treated groups. During this period, the signal remained in KC and SEC from the nontreated IR group (Fig. 5). To confirm cell identity, CD68- and CD34-specific labeling of KC and SEC, respectively, was performed as described in the Materials and Methods section and visualized through light microscopy (Fig. 6). As shown in Fig. 5, during the first postreperfusion hour, SEC and KC expressed intensively the marker (+++), which was not found in the hepatocytes (−); at 4 h, expression of the carbonyl groups was similar in the studied populations (++/+++), and at 24 h, expression persisted in the SEC and KC (++) and was negative in the hepatocytes. As an effect of the IR injury, ROS are released that reach the

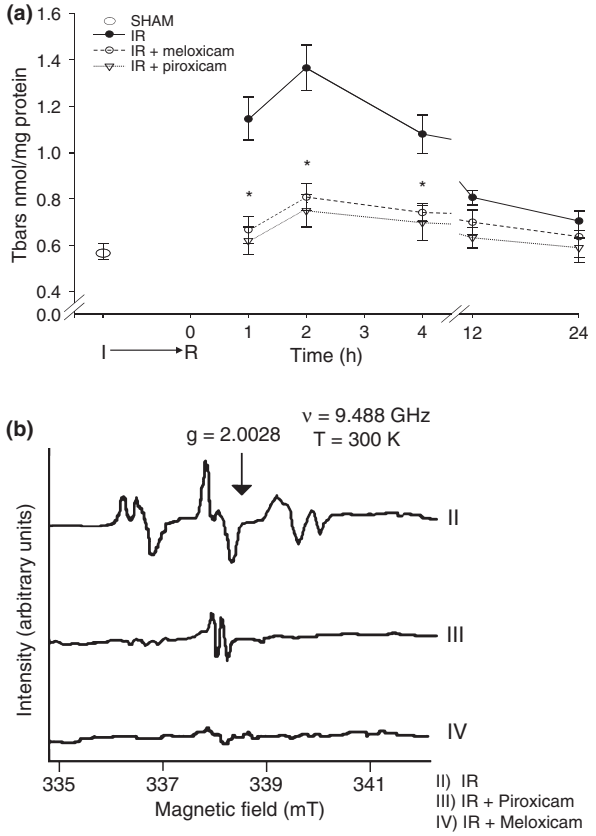

Figure 3 (a) Liver thiobarbituric-acid reactive substance (TBARS) content. In the sham group (I), a basal value of 0.58 ± 0.3 was obtained, whereas in the ischemia–reperfusion (IR) group without treatment (II), the presence of TBARS was higher after 1, 2, and 4 h, compared with COX-1 (III)- and COX-2 (IV)-treated groups; statistical difference is indicated by the asterisk. No significant difference was found between nonsteroidal anti-inflammatory drugs (NSAIDs)-treated groups. A molar extinction coefficient of 1.56×10^5/M/cm was used to estimate values. (b) Electron paramagnetic resonance (EPR). We used the free radicals spin trap alpha-phenyl *N*-tert-butylnitrone (PBN) to detect reactive oxygen species (ROS) directly in bile samples obtained after ischemia. As a control, we analyzed the samples of the sham group (I) with and without PBN, and the samples of each experimental group without PBN. No additional ROS could be detected in these groups (data not shown). In the groups under IR, a decline in signal intensity in NSAIDs-treated groups was observed (groups III and IV) compared with the nontreated IR group (II). Only a small spectral feature centered on 2.0028 g (arrow) could be detected in these samples whose spectral properties and possible nature are described in the Results section (data not shown). Spectra were obtained from IR (II), IR + piroxicam (III), and IR + meloxicam (IV) samples. EPR parameters were as described in the Materials and Methods section.

portal and systemic circulation; this event was demonstrated by the expression of carbonylation in liver SEC; as the injury progresses, it extends to the KC because of their protective function. Other studies have demonstrated the participation of endothelial and Kupffer cells, but in an indirect manner; the applied immunohistochemistry (PC) demonstrated *in vivo* the damage to these cells.

Apoptosis during liver ischemia–reperfusion

As shown in Fig. 7, TUNEL-positive cells were rarely found in the liver treated with piroxicam and meloxicam compared with the IR group. In the sham group, one or two cells were found, which was considered a normal finding. The most relevant data were obtained after 4 h of reperfusion. Brown-colored cells were considered positive for apoptosis, and a few red cells were observed in the sinusoidal space.

Discussion

The model used reproduces the main events found in the clinical practice of the Surgeon and Gastroenterologist interested in the liver as, for example, in porto-hepatic ischemia induced by the Pringle maneuver [41,42], with its modifications or indications according to each case, or under all conditions that reduce arterial and/or venous flow [43–47].

A striking fact of the results as a whole is that once a change was detected in one of the assayed hepatic injury indicators, a similar variation in time and magnitude occurred in the remaining liver-damage indicators. These changes emerged previously, and were quantitatively higher in the IR group than in NSAIDs-treated animals (compare, for example, data from Figs 1 and 5), but a close correlation among these is clear, mainly during the first 4 h postreperfusion. These synchronized points suggest a cellular response to ischemia–reperfusion that is apparently triggered by a burst in ROS production, followed by a domino effect that spreads the injury in an amplification cascade. KC activation during the initial reperfusion period appears to cause the sudden generation of ROS once restoration of blood flow occurs [6,48].

Our data on PC are in agreement with evidence that the initial damage occurs in KC, and additionally in SEC (Fig. 5a). The ROS burst impinges upon cellular constituents, such as protein and lipids, to establish oxidative stress in which ROS generation surpasses cellular mechanisms to promote their disappearance. Moreover, activated KC generates primary cytokines that enhance KC activation and promote neutrophil recruitment into the liver, which can create a vicious circle that further increased the ROS pool [6,47,49,50]. This higher ROS pool was manifested by a progressive accumulation of PC observed in KC and SEC and later, in hepatocytes (Fig. 5

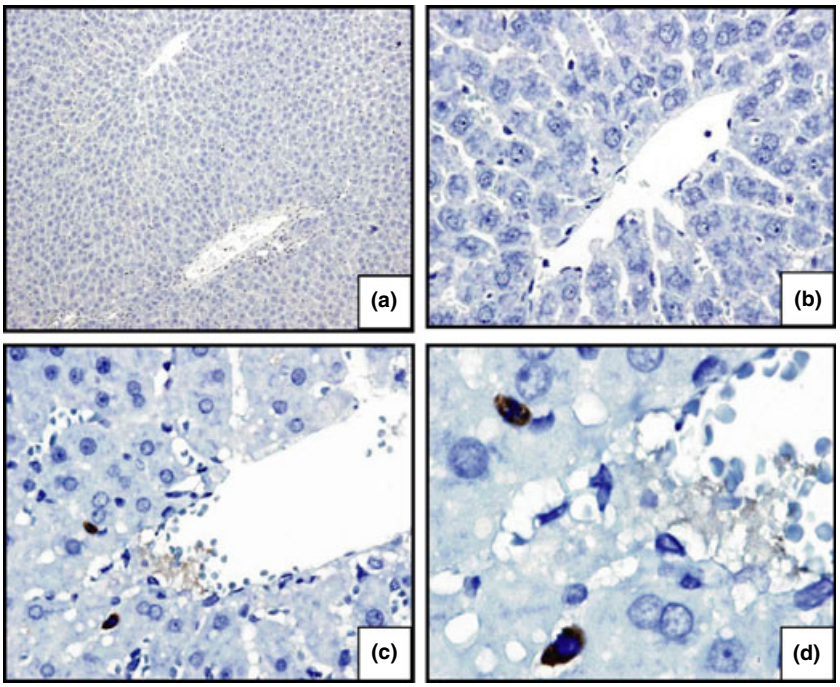

Figure 4 Liver expression of protein carbonylation at the end of ischemia time. The sham group showed normal histopathology in one portal triad (a) and central vein (b), sinusoidal endothelial cells (SEC), and Kupffer cells (KC), and hepatocytes were negative to staining. In contrast, liver samples from the nontreated IR group (II) after 90 min of ischemia showed staining in KC (c, d). These samples were taken prior to the reperfusion phase. This observation was not found in animals from groups III and IV. Amplification, 100× (a), 40× (b, c), and 20× (d).

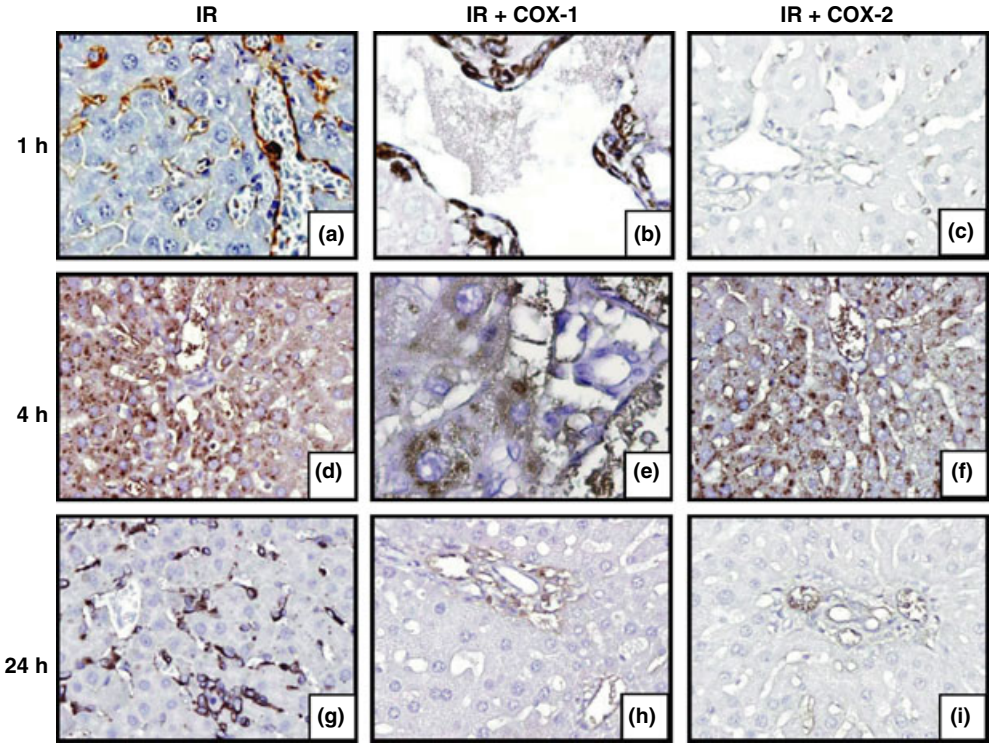

Figure 5 Liver expression of protein carbonylation (PC) after reperfusion. After 1 h of reperfusion, the untreated IR group showed (a) PC in sinusoidal endothelial cells (SEC) +++ and Kupffer cells (KC) +++. In contrast, livers treated with COX-1 and -2 inhibitors showed (b) PC in SEC ++ and (c) SEC +, respectively. After 4 h of reperfusion (d, e, f), we observed PC in SEC, CK, and hepatocytes (HE) ++/+++. At 24 h of reperfusion, liver samples were characterized by (g) PC in SEC and CK ++. (h, i) PC in SEC ++. Amplification, 100× (f), 40× (b), and 20× (a, c, d, e, g, h, i).

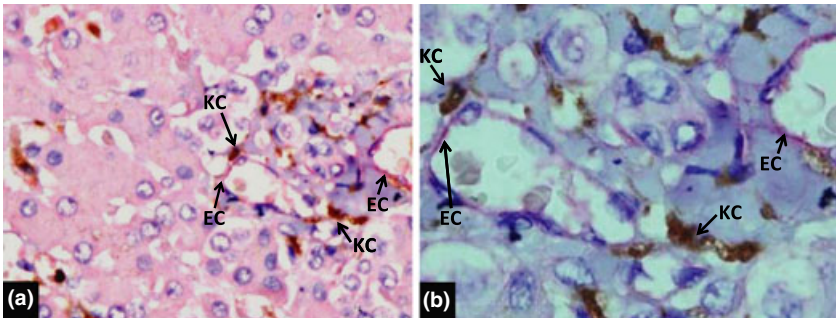

Figure 6 Immunohistochemistry to CD34 and -68. Liver samples of a portal space showed immune expression, red to sinusoidal endothelial cells (SEC) and brown to Kupffer cells (KC). Amplification, 40× (a) and 100× (b).

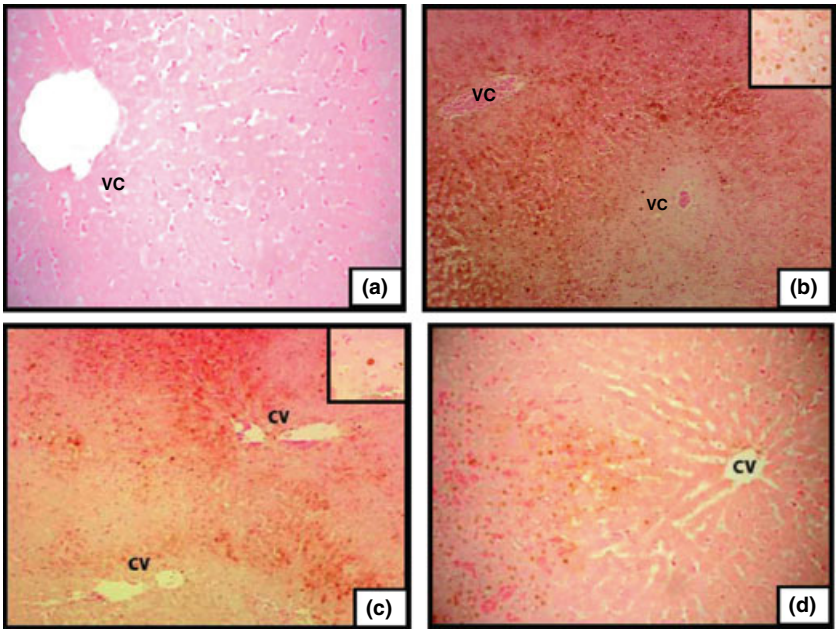

Figure 7 Terminal deoxynucleotidyl transferase (TdT)-mediated dUTP nick-end labeling (TUNEL) technique. In the sham group (a), 5 ± 2 apoptotic cells are observed per Portal space (PS). Statistically significant differences were found when comparing the untreated group with that which underwent hepatic ischemia–reperfusion (IR) (b), observing 101 ± 35 apoptotic cells per PS vs. 41 ± 11 apoptotic cells per PS in the hepatic IR + piroxicam (c) and vs. 37 ± 6 observed in the hepatic IR + meloxicam (d). No statistical difference was found between groups III and IV. Amplification, 40× and 10×, respectively.

d–f). Following this line of thought, ROS reached lipids in cell membranes for promoting enhanced production of TBARS (Fig. 3a) and in the ROS pool of ROS directly measured in bile (Fig. 3b). ROS-mediated injury to proteins and lipids leads to cell necrosis (Fig. 2), apoptosis and more rapid release of hepatic enzymes from parenchymal cells to serum (Fig. 1).

Lipids in the hepatic tissue were assessed by the formation of TBARS adducts; this is not a specific method for the affected lipids, but it provided the amount of oxidized lipids needed in the analyzed samples. These results were evident from the first hour; they reached their maximal biochemical expression within the 2–4 postreperfusion hours (Fig. 3a). Decline started at approximately 24 h, which could be due to wearing out of the oxidizable sources or a halt in their release caused by apoptosis or necrosis [16].

Notwithstanding this, the relevant finding in this work comprised the ability of piroxicam and meloxicam to lower ROS levels, presumably at the level of KC and SEC, during the initial reperfusion period. Data from Fig. 4 are relevant because they demonstrate that PC occurs at the very beginning of reperfusion in untreated rats, whereas in COX-treated groups, PC presented only at a later stage and with much lower severity. The present results suggest that PC does not comprise solely another of the deleterious and causative agents in ischemic hypoxic tissue damage, but rather, that it is probably one that underlies many of the important events observed (Fig. 5); in order to describe the generation of protein, carbonyls are formed by a direct metal-catalyzed oxidative attack on the amino acid side chains of proline, arginine, lysine, and threonine. In addition, carbonyl derivatives on lysine, cysteine, and histidine can be formed by secondary reactions with reactive carbonyl compounds on carbohydrates (glycoxidation products), lipids, and advanced glycation/lipoxidation end-products [19]. Some diseases have been associated with PC such as Alzheimer, Parkinson, diabetes, sepsis, cancer, and others [20–22].

The usefulness of this finding lies in the possibility of correlating it with serum enzyme values, apoptosis index by TUNEL, and ROS (MDA, EPR), which could indicate progression of the damage. This would allow using this parameter as a tissue monitoring tool with clinical significance [22,51–53].

In summary, the anti-inflammatory-mediated ability to lower ROS values also decreased PC, TBARS, EPR signal in bile, necrosis, apoptosis, and release of hepatic enzymes in serum. No experiment was carried out to define specifically whether this effect was mainly a result of a preventive action of NSAIDs on ROS generation, or whether it was by an effect of the drugs in promoting ROS disappearance. Importance was given to describe a hepato-protective action of two NSAIDs at least during the initial 24 h after reperfusion. These results are in agreement with our previous work that showed a hepato-protective action of other NSAIDs in preventing certain deleterious effects of acute ethanol intoxication [30–32]. The hepato-protective action of aspirin on acetaminophen-induced liver injury has been reported by other authors [54,55]. In this regard, the work of Imaeda *et al.* is also of relevance, because the authors found that the action of aspirin was due to the down-regulation of pro-inflammatory cytokines [56]. In addition, this group identified the requirement of Tlr9 and the Nalp3 inflammasome for acetaminophen-induced hepatotoxicity.

Recently, Hamada *et al.* showed, in COX-2-deficient mice, significantly decreased levels of IL-2, as well as of IL-12, a cytokine known to play a central role in Th1 effector cell differentiation [57]; previously, Ozturk and Gezici showed that Celexoxib has beneficial effects in IR injury and may protect the liver [58]; these data correlate with our findings in this experimental study.

Further experiments are required with drugs from the anti-inflammatory pharmacologic group in order to define the compound with fewest contraindications and adverse effects that could be utilized as the elective hepato-protective compound [59–62]. The use of such a putative compound could be of particular usefulness in programmed cases of ischemia–reperfusion. As damage occurs from the first hour and is proportional to the duration of the ischemic event, the effects on the function and viability of the liver will depend on the timeliness and effectiveness of the pharmacologic intervention.

Authorship

M-JEE, O-SJA, JD, H-MR, and PE designed research/study; M-JEE, and O-SJA performed research/study; JD, ME, GR, H-MR, CA, M-ACE, M-JEE, O-SJA, C-DC, and PE contributed important reagents; M-JEE, O-SJA, C-DD, JD, ME, H-MR, CA, M-ACE, ME, and GR collected data; M-JEE, and PE analyzed data and wrote the paper.

Funding

The authors have declared no funding.

Acknowledgements

The authors thank Benjamín León, Andrés Montiel-Rodríguez, Carolina Baños-Galeana, Carmen Peña-Jiménez, Mario Téllez-Sánchez, Jorge García-Loya, and Graciela Villeda-Rodríguez (Department of Surgery, Faculty of Medicine (FM)-UNAM) for technical assistance in animal care and MDA samples, and Beatriz Hernández for performing the TUNEL assay (Department of Cell and Tissue Biology, FM-UNAM). We also thank Dr. Fernando Villegas-Álvarez, Professor of Surgery, FM-UNAM. The cerebral sample was donated by Dr. Jesús D. Rembao-Bojórquez, Head of the Department of Pathology at the Instituto Nacional de Neurología y Neurocirugía (INNN) in Mexico City. Dr. E.E. Montalvo-Javé received grants from CONACyT-México and DGEP-UNAM (Mexico).

References

1. Montalvo-Javé EE, Escalante-Tattersfield T, Ortega-Salgado JA, Piña E, Geller DA. Factors in the pathophysiology of the liver ischemia-reperfusion injury. *J Surg Res* 2008; **147**: 153.
2. Bilzer M, Gerbes AL. Preservation injury of the liver: mechanisms and novel therapeutic strategies. *J Hepatol* 2000; **32**: 508.
3. Wisse E, De Zanger RB, Charels K, Van Der Smissen P, McCuskey RS. The liver sieve: considerations concerning the structure and function of endothelial fenestrae, the sinusoidal wall and the space of Disse. *Hepatology* 1985; **5**: 683.
4. Caldwell-Kenkel JC, Currin RT, Tanaka Y, Thurman RG, Lemasters JJ. Reperfusion injury to endothelial cells following cold ischemic storage of rat livers. *Hepatology* 1989; **10**: 292.
5. McKeown CM, Edwards V, Phillips MJ, Harvey PR, Petrunka CN, Strasberg SM. Sinusoidal lining cell damage: the critical injury in cold preservation of liver allografts in the rat. *Transplantation* 1988; **46**: 178.
6. Jaeschke H. Molecular mechanisms of hepatic ischemia-reperfusion injury and preconditioning. *Am J Physiol Gastrointest Liver Physiol* 2003; **284**: G15.
7. Kim JS, Jin Y, Lemasters JJ. Reactive oxygen species, but not Ca2+ overloading, trigger pH- and mitochondrial permeability transition-dependent death of adult rat myocytes after ischemia-reperfusion. *Am J Physiol Heart Circ Physiol* 2006; **290**: H2024.

8. Mosher B, Dean R, Harkema J, Remick D, Palma J, Crockett E. Inhibition of Kupffer cells reduced CXC chemokine production and liver injury. *J Surg Res* 2001; **99**: 201.
9. Serracino-Inglott F, Habib NA, Mathie RT. Hepatic ischemia-reperfusion injury. *Am J Surg* 2001; **181**: 160.
10. Sindram D, Porte RJ, Hoffman MR, Bentley RC, Clavien PA. Platelets induce sinusoidal endothelial cell apoptosis upon reperfusion of the cold ischemic rat liver. *Gastroenterology* 2000; **118**: 183.
11. Gao W, Bentley RC, Madden JF, Clavien PA. Apoptosis of sinusoidal endothelial cells is a critical mechanism of preservation injury in rat liver transplantation. *Hepatology* 1998; **27**: 1652.
12. Dubois RN, Abramson SB, Crofford L, *et al.* Cyclooxygenase in biology and disease. *FASEB J* 1998; **12**: 1063.
13. Turnage RH, Kadesky KM, Bartula L, Myers SI. Pulmonary thromboxane release following intestinal reperfusion. *J Surg Res* 1995; **58**: 552.
14. Hossain MA, Wakabayashi H, Izuishi K, Okano K, Yachida S, Maeta H. The role of prostaglandins in liver ischemia-reperfusion injury. *Curr Pharm Des* 2006; **12**: 2935.
15. Arii S, Teramoto K, Kawamura T. Current progress in the understanding of and therapeutic strategies for ischemia and reperfusion injury of the liver. *J Hepatobiliary Pancreat Surg* 2003; **10**: 189.
16. Jaeschke H, Lemasters JJ. Apoptosis versus oncotic necrosis in hepatic ischemia/reperfusion injury. *Gastroenterology* 2003; **125**: 1246.
17. Wood KC, Gladwin MT. The hydrogen highway to reperfusion therapy. *Nat Med* 2007; **13**: 673.
18. Malhi H, Gores GJ, Lemasters JJ. Apoptosis and necrosis in the liver: a tale of two deaths? *Hepatology* 2006; **43**: S31.
19. Nystrom T. Role of oxidative carbonylation in protein quality control and senescence. *EMBO J* 2005; **24**: 1311.
20. Levine RL. Carbonyl modified proteins in cellular regulation, aging, and disease. *Free Radic Biol Med* 2002; **32**: 790.
21. Dalle-Donne I, Giustarini D, Colombo R, Rossi R, Milzani A. Protein carbonylation in human diseases. *Trends Mol Med* 2003; **9**: 169.
22. Dalle-Donne I, Aldini G, Carini M, Colombo R, Rossi R, Milzani A. Protein carbonylation, cellular dysfunction, and disease progression. *J Cell Mol Med* 2006; **10**: 389.
23. Wang D, Mann JR, DuBois RN. The role of prostaglandins and other eicosanoids in the gastrointestinal tract. *Gastroenterology* 2005; **128**: 1445.
24. Morham SG, Langenbach R, Loftin CD, *et al.* Prostaglandin synthase 2 gene disruption causes severe renal pathology in the mouse. *Cell* 1995; **83**: 473.
25. Berg DJ, Zhang J, Weinstock JV, *et al.* Rapid development of colitis in NSAID-treated IL-10-deficient mice. *Gastroenterology* 2002; **123**: 1527.
26. Smith WL, Meade EA, DeWitt DL. Interactions of PGH synthase isozymes-1 and -2 with NSAIDs. *Ann N Y Acad Sci* 1994; **744**: 50.
27. Pairet M, van Ryn J, Schierok H, Mauz A, Trummlitz G, Engelhardt G. Differential inhibition of cyclooxygenases-1 and -2 by meloxicam and its 4′-isomer. *Inflamm Res* 1998; **47**: 270.
28. Zentella de Piña M, Sandoval-Montiel A, Serrano-Alessandri L, Montalvo-Javé E, Zentella-Dehesa A, Piña E. Ethanol-mediated oxidative changes in blood lipids and proteins are reversed by aspirin-like drugs. *Arch Med Res* 2007; **38**: 269.
29. Saldaña-Balmori Y, Zentella de Piña M, Guinzberg R, Rocha-Hernández A, Piña E. Piroxicam modifies the effects of ethanol on isolated rat hepatocytes. *Eur J Pharmacol* 1996; **317**: 225.
30. Zentella de Piña M, Corona S, Rocha-Hernández AE, Saldaña-Balmori Y, Cabrera G, Piña E. Restoration by piroxicam of liver glutathione levels decreased by acute ethanol intoxication. *Life Sci* 1994; **54**: 1433.
31. Zentella de Piña M, Saldaña-Balmori Y, Hernández-Tobias A, Piña E. Nonsteroidal antiinflammatory drugs lower ethanol-mediated liver increase in lipids and thiobarbituric acid reactive substances. *Alcohol Clin Exp Res* 1993; **17**: 1228.
32. Zentella de Piña M, Hernández-Tobias A, Saldaña-Balmori Y, Díaz-Belmont A, Piña E. Biochemical ethanol effects affected by a non-steroidal anti-inflammatory drug. *FEBS Lett* 1992; **298**: 123.
33. Hernández-Muñoz R, Díaz-Muñoz M, Suárez J, Chagoya de Sánchez V. Adenosine partially prevents cirrhosis induced by carbon tetrachloride in rats. *Hepatology* 1990; **12**: 242.
34. Ikeda T, Yanaga K, Kishikawa K, Kakizoe S, Shimada M, Sugimachi K. Ischemic injury in liver transplantation: difference in injury sites between warm and cold ischemia in rats. *Hepatology* 1992; **16**: 454.
35. Ishak K, Baptista A, Bianchi L, *et al.* Histological grading and staging of chronic hepatitis. *J Hepatol* 1995; **22**: 696.
36. Wilbur KM, Bernheim F, Shapiro OW. The thiobarbituric acid reagent as a test for the oxidation of unsaturated fatty acids by various agents. *Arch Biochem* 1949; **24**: 305.
37. Smith MA, Sayre LM, Anderson VE, *et al.* Cytochemical demonstration of oxidative damage in Alzheimer disease by immunochemical enhancement of the carbonyl reaction with 2,4-dinitrophenylhydrazine. *J Histochem Cytochem* 1998; **46**: 731.
38. Corona-Morales AA, Castell A, Zhang L. L-DOPA-induced neurotoxic and apoptotic changes on cultured chromaffin cells. *Neuroreport* 2000; **11**: 503.
39. Wright G, Terada K, Yano M, Sergeev I, Mori M. Oxidative stress inhibits the mitochondrial import of preproteins and leads to their degradation. *Exp Cell Res* 2001; **263**: 107.
40. Díaz-Juárez J, Rivera-Valerdi L, Bernal-Cerrillo DE, Hernández-Muñoz R. Predominance of released mitochondrial enzymes by partial hepatectomy-induced rat regenerating

liver is controlled by hemodynamic changes and not related to mitochondrial damage. *Scand J Gastroenterol* 2006; **41**: 223.
41. Pringle JH. V. Notes on the arrest of hepatic hemorrhage due to trauma. *Ann Surg* 1908; **48**: 541.
42. Garcea G, Gescher A, Steward W, Dennison A, Berry D. Oxidative stress in humans following the Pringle manoeuvre. *Hepatobiliary Pancreat Dis Int* 2006; **5**: 210.
43. Richardson JD. Changes in the management of injuries to the liver and spleen. *J Am Coll Surg* 2005; **200**: 648.
44. Tsung A, Geller DA. Workup of the incidental liver lesion. *Adv Surg* 2005; **39**: 331.
45. Belghiti J, Noun R, Malafosse R, *et al.* Continuous versus intermittent portal triad clamping for liver resection: a controlled study. *Ann Surg* 1999; **229**: 369.
46. Clavien PA, Emond J, Vauthey JN, Belghiti J, Chari RS, Strasberg SM. Protection of the liver during hepatic surgery. *J Gastrointest Surg* 2004; **8**: 313.
47. Selzner N, Rudiger H, Graf R, Clavien PA. Protective strategies against ischemic injury of the liver. *Gastroenterology* 2003; **125**: 917.
48. Caldwell-Kenkel JC, Currin RT, Tanaka Y, Thurman RG, Lemasters JJ. Kupffer cell activation and endothelial cell damage after storage of rat livers: effects of reperfusion. *Hepatology* 1991; **13**: 83.
49. Cavalieri B, Mosca M, Ramadori P, *et al.* Neutrophil recruitment in the reperfused-injured rat liver was effectively attenuated by repertaxin, a novel allosteric noncompetitive inhibitor of CXCL8 receptors: a therapeutic approach for the treatment of post-ischemic hepatic syndromes. *Int J Immunopathol Pharmacol* 2005; **18**: 475.
50. Colletti LM, Kunkel SL, Walz A, *et al.* The role of cytokine networks in the local liver injury following hepatic ischemia/reperfusion in the rat. *Hepatology* 1996; **23**: 506.
51. Frank J, Pompella A, Biesalski HK. Histochemical visualization of oxidant stress. *Free Radic Biol Med* 2000; **29**: 1096.
52. Fukai M, Hayashi T, Yokota R, *et al.* Lipid peroxidation during ischemia depends on ischemia time in warm ischemia and reperfusion of rat liver. *Free Radic Biol Med* 2005; **38**: 1372.
53. Grimsrud PA, Xie H, Griffin TJ, Bernlohr DA. Oxidative stress and covalent modification of protein with bioactive aldehydes. *J Biol Chem* 2008; **283**: 21837.
54. De Vries J, De Jong J, Lock FM, Van Bree L, Mullink H, Veldhuizen RW. Protection against paracetamol-induced hepatotoxicity by acetylsalicylic acid in rats. *Toxicology* 1984; **30**: 297.
55. Wu KK. Aspirin and other cyclooxygenase inhibitors: new therapeutic insights. *Semin Vasc Med* 2003; **3**: 107.
56. Imaeda AB, Watanabe A, Sohail MA, *et al.* Acetaminophen-induced hepatotoxicity in mice is dependent on Tlr9 and the Nalp3 inflammasome. *J Clin Invest* 2009; **119**: 305.
57. Hamada T, Tsuchihashi S, Avanesyan A, *et al.* Cyclooxygenase-2 deficiency enhances Th2 immune responses and impairs neutrophil recruitment in hepatic ischemia/reperfusion injury. *J Immunol* 2008; **180**: 1843.
58. Ozturk H, Gezici A. The effect of celecoxib, a selective COX-2 inhibitor, on liver ischemia/reperfusion-induced oxidative stress in rats. *Hepatol Res* 2006; **34**: 76.
59. Warner TD, Mitchell JA. COX-2 selectivity alone does not define the cardiovascular risks associated with non-steroidal anti-inflammatory drugs. *Lancet* 2008; **371**: 270.
60. Targownik LE, Metge CJ, Leung S, Chateau DG. The relative efficacies of gastroprotective strategies in chronic users of nonsteroidal anti-inflammatory drugs. *Gastroenterology* 2008; **134**: 937.
61. Strand V. Are COX-2 inhibitors preferable to non-selective non-steroidal anti-inflammatory drugs in patients with risk of cardiovascular events taking low-dose aspirin? *Lancet* 2007; **370**: 2138.
62. Warner TD, Vojnovic I, Bishop-Bailey D, Mitchell JA. Influence of plasma protein on the potencies of inhibitors of cyclooxygenase-1 and -2. *FASEB J* 2006; **20**: 542.